Use of ResNets for HLB Disease Detection on Orange Leaves Using Terrestrial Multispectral Images

Letícia Rosim Porto[1], Florent Abdelghafour [2], Maurycio Oviedo[1], Nilton Nobuhiro Imai[1], Antonio Maria Garcia Tommaselli[1], Ryad Bendoula[2]

[1] São Paulo State University (UNESP), Presidente Prudente, Brazil – (leticia.porto, maurycio.oviedo, nilton.imai, a.tommaselli)@unesp.br
[2] INRAE, Institut Agro, ITAP, University of Montpellier, 34196, Montpellier, France – (florent.abdelghafour, ryad.bendoula)@inrae.fr

Keywords: Deep Learning, Convolutional Neural Network (CNN), Digital Agriculture, Huanglongbing, High Resolution, Proximal Remote Sensing.

Abstract

Huanglongbing (HLB) is a bacterial disease transmitted by different vectors of sap-sucking insects. It affects all crops of citrus trees, decreasing the values of those fruits in the market and eventually the decay of orchards. In Brazil, the world's leading orange producer, citriculture faces severe issues with HLB and substantial economic loss. Technical means of scanning the orchards with high-throughput becomes essential for the sustainability of this industry. In this study, we propose to investigate an operational strategy consisting of scanning large portions of foliage (the canopy of one tree or more) in which there can few early foliage symptoms. It is proposed to investigate deep learning tools to solve this complex binary classification problem. The study is based on a dataset comprising 1,297 terrestrial multispectral (14 channels) images captured at high spatial resolution in a commercial orange orchard in Brazil. It is proposed to adapt and retrain standard neural network architectures, namely ResNets18 and ResNets34, to process such images. Our analysis reveals promising results, with both models demonstrating convergence and achieving stable performance. Notably, ResNet18 outperformed ResNet34, achieving an accuracy of 76.45% compared to 66.79% from ResNet34. These findings suggest that deep neural network methods can effectively manage non-radiometrically calibrated data and accurately distinguish images with HLB symptoms from healthy plants . However, with reduced datasets and limited possibilities for transfer learning and fine-tuning, it seems that only reasonable sized networks can be trained. Thus, more advanced state-of-the-art tools of the are still challenging to deploy for agricultural multi-or hyperspectral data.

1. Introduction

Brazil is the major orange producer and the largest exporter of concentrated orange juice worldwide. However, orange orchards, especially in the São Paulo State and the southwest of the Minas Gerais State suffer from a high pathogenic pressure. It is estimated that 38% of orange trees are infected by Huanglongbing (HLB), the most destructive disease in citriculture and a major threat to the industry (Fundecitrus, 2023). The most common HLB symptom is asymmetrical yellow spots on the leaves. This symptom can occur in any branch of the citrus tree, including the lateral ones. HLB infections result in significant yield loss, decay of tree population or severe decrease in the fruit quality and global marketability (Alquézar et al., 2022; Bové, 2006).

A proficient disease detection system can help prevent economic losses and safeguard food security. In the absence of such a system, continuous monitoring of entire areas by highly skilled technicians is often unfeasible. Furthermore, distinguishing among the various diseases and nutritional deficiencies that can often be confused with HLB, poses a significant challenge (Barbedo et al., 2018). In the absence of efficient crop protection methods, HLB-infected trees are often cut down and removed from plots as soon as symptoms are detected to prevent epidemic outbursts. There is a recognised need for high-throughput scanning and detection systems to detect the very first occurrence of infection within orchards.

Image proximal sensing for agricultural application is a scientific subject that is on the rise and has shown great potential in perennial crops. In this particular case the main information is found in the lateral face and thus observable with a ground view rather than an top-down on aerial view. On the other hand, acquiring terrestrial images under natural lighting conditions poses several issues because of the non-uniform illumination in natural environment. Image acquisition in fruit orchards is even harder due to variations in lighting and tree canopy geometry, resulting in complex acquisition (Rançon et al., 2023; Deng et al., 2019; Aquino et al., 2018; Wendel et al., 2018; Wendel & Underwood, 2017; Underwood et al., 2016; Deery et al., 2014).

Radiometric calibration is usually required to settle the problem of lighting variation, especially for spectral imaging, where the specific signatures are key information to determine the presence of symptoms in the canopy. However, the use of radiometric calibration panels can be impractical when monitoring large crop areas. In this context, conventional processing methods based on linear algebra (*e.g.* chemometrics) (Wold, 1995) are known to be sensitive to these variations. However, more complex and non-linear models, such as deep learning, could overcome the lack of inconsistent radiometry. With sufficient datasets combined with data-augmentation or even transfer learning, deep-learning has shown great potential for processing raw and heterogeneous data (Kamilaris & Prenafeta-Boldú, 2018).

Given this perspective, the contribution of this work consists of a practical implementation of deep learning for a binary detection

This contribution has been peer-reviewed. The double-blind peer-review was conducted on the basis of the full paper.
https://doi.org/10.5194/isprs-annals-X-3-2024-331-2024 | © Author(s) 2024. CC BY 4.0 License.

problem using multispectral images acquired under complex conditions. The aim of this paper is to analyse the viability of using deep neural networks to classify multispectral images between HLB-infected and non-HLB canopies *in situ*. In this practical context, it is difficult to grade symptoms or estimate the proportions of infected areas. The challenge is to detect the presence of the disease regardless of the state of infection or its severity or whenever it possible, with early symptoms, *i.e.* when only a few leaves are affected within a large portion of healthy canopy. To perform this task, we compare two variants of the ResNet architecture, with 18 and 34 layers, which we adapted to multispectral images.

2. Background

2.1 ResNet

ResNet, short for Residual Network, is a type of deep neural network architecture introduced in 2016. It represents a significant advancement in the design of Convolutional Neural Networks (CNNs), particularly for tasks such as image classification and object detection. It enables to cope with issues of overfitting and gradient vanishing, which is essential when working with spectral images of smaller and less diverse datasets. Distinguished by incorporating skip connections and the consistent application of batch normalisation layers following each convolutional operation, these architectural enhancements were devised to facilitate the training of exceedingly deep CNNs, exemplified by ResNet-18 and ResNet-34, featuring 18 and 34 convolutional layers, respectively. Training in ImageNet dataset, the ResNet34 exhibited considerably lower training error and was generalisable to the validation data. This indicated that the degradation problem was well addressed in this setting and managed to obtain accuracy gains from increased depth (He et al., 2016).

Training a deep neural network with a dataset containing exotic data (*i.e.* for which there is no pre-trained version nor comparable databases in terms neither of spatial dimension, nor spectral depth) for binary classification (example, HLB vs. non-HLB) is an arduous task. Distinguishing between foliage containing only healthy leaves form those with HLB symptoms within a complex canopy, especially under varying light in outdoor conditions is a challenging task. Typically, deep learning yields favourable results due to transfer learning and fine-tuning. However, because of the exotic nature of the data (multispectral, canopy, and disease symptoms), transfer learning and fine-tuning are not straightforward.

2.2 Disease detection using deep learning

Recently, Shafik et al. (2024) conducted experiments in the search for the classification of diseases in plants through images. In their results, an accuracy of 97.79% was achieved. However, there still exists uncertainty in the identification or classification of the disease in the early signs of green attack.

Rangarajan & Purushothaman (2020), using RGB and YCbCr images, proposed disease detection using ResNet (16, 50, 101, 152). Despite the limitation of the dataset, they were able to achieve an accuracy of 99.4% in their work. Furthermore, it is noticeable that the colours affect the accuracy of specific disease classification, and due to the complexities of the problem, overfitting may occur during the training process.

Additionally, Mostafa Ahmed & Ali Ahmed (2023) approached the use of the ResNet50 model, among others, to detect diseases in palm leaves. The study achieved an accuracy of 99.23% using the CNN model to classify the various known diseases in palm trees. The authors also addressed challenges such as variation of luminance, background differences, image scale variations, and inter-class similarity in palm tree disease classification.

In the identification of HLB in citrus trees, current studies focus on identifying the disease using individual leaves rather than in their field context (Yang et al., 2021, Qiu et al., 2022). Additionally, some studies test field issues as proposed by Dhiman et al. (2023), but the analysis was conducted on the fruit images and not on the leaf symptoms.

3. Method

3.1 Data acquisition and preprocessing

Image acquisition was performed on a commercial orange producing farm located in the north of São Paulo State, in Brazil. The images were acquired between August 15th and 18th, 2023, in a 9 ha plot of sweet orange Pera Rio (*Citrus sinesis* (L.) Osbeck) with three years old. Two classes of images were acquired: first, plants with HLB-symptomatic leaves and, then, plants with only healthy leaves. The HLB-symptomatic plants were previously identified by a trained team of technicians who inspected each tree walking along rows or on a platform over a tractor. The area covered by each image is then comparable to the scale at which the monitoring for pathology is conducted.

Figure 1.a presents an example of orange leaves with HLB symptoms characterised by asymmetrical yellow spots. Figure 1.b shows the laborious and time-consuming task of visual inspection walking in oranges orchards.

Figure 1. a) Orange leaves with HLB symptoms. b) Visual inspection of HLB infection in a commercial orange orchard.

The images acquisition was conducted using the Sony Alpha 7R2 Sextuple Multispectral Camera developed by Agrowing. The camera's sensor frame is divided into six parts to acquire the same scene in 14 bands through six camera heads (lenses), with the following spectral bands: 405, 430, 450, 490, 525, 550, 560, 570, 630, 650, 685, 710, 735 and 850 nm. The bandwidth is 25 nm for visible channels, 15 nm for red-edge channels and 10 nm for the near-infrared channel (Agrowing, 2024).

The dataset contains images with noticeable illumination variability. The acquisition was conducted with variations in the shutter speed in the camera setup. This approach provides a dataset with real examples of high illumination and radiometric variability. It also enabled a rich basis of data augmentation in the radiometrical dimension. This is an important increment, since the traditional data augmentation methods mostly focus on spatial dimensions.

This contribution has been peer-reviewed. The double-blind peer-review was conducted on the basis of the full paper.
https://doi.org/10.5194/isprs-annals-X-3-2024-331-2024 | © Author(s) 2024. CC BY 4.0 License.

Figure 2 illustrates the Agrowing camera (Figure 2.a), the image acquisition (Figure 2.b), and the imaging preprocessing (Figure 2.c). The raw images were preprocessed using the camera manufacturer's software AwBasic. Each frame was cropped, resulting in images sized at 2552 x 2560 pixels.

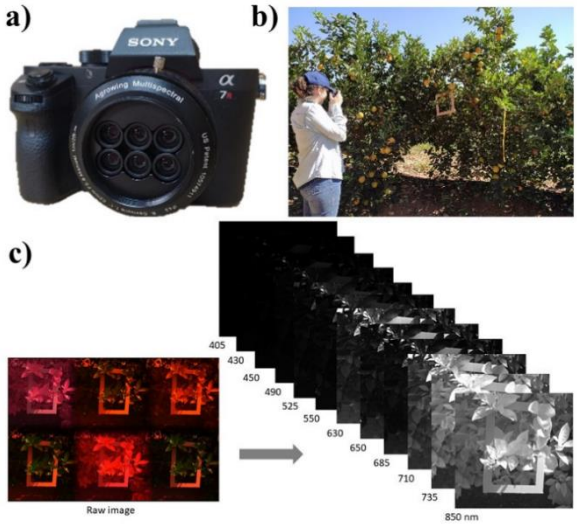

Figure 2. a) Sony Alpha 7R2 Sextuple Multispectral Camera. b) Terrestrial acquisition of images in the orange orchard. c) Illustration of the extraction of 14 monochromatic images from multispectral raw image.

3.2 Dataset

The dataset consists of a total of 1,297 multispectral images, which have been labelled as HLB (865 multispectral images infected) and non-HLB (432 multispectral images non-infected). Given that each multispectral image contains 14 monochromatic 8-bits images, the dataset comprises a total of 18,158 images.

Data labeling was done in terms of image based on information acquired in the orchard (pre-identification of HLB symptomatic trees and acquisition time). The image files were split into two folders: HLB and non-HLB images. The dataset was created using Hierarchical Data Format version 5 (hdf5) format containing all the dataset with its metadata and the necessary information for labelling and data splitting. The images were subsampled to 1276 x 1280 pixels by nearest neighbour interpolation.

The dataset was randomly divided into two smaller datasets: the training dataset and the test dataset. The training and test datasets consist, respectively, of 80% and 20% data of the original one. The images are distributed equally between the 14 spectral channels.

3.3 Configuration of the models

ResNet18 and ResNet34 were used to classify images between HLB and non-HLB. It is assumed that the deeper the network, the more layers and parameters will be optimised, allowing a more complex model and potentially a better discrimination if the data are rich enough.

The models were firstly trained with the training dataset. Table 1 shows the hyperparameters used to configure the training phase of the classification models in this work. The ResNet18 architecture had 11,474,754 trainable parameters, while ResNet34 had 21,582,914 trainable parameters. The models were then tested with the test dataset.

Hyperparameter Name	Value
Batch size	8
Number of epochs	200
Optimisation algorithm	Adam
Loss function	Cross Entropy
Metric	Accuracy
Learning rate	0.001
Momentum	None
Activation function in convolutional layer	ReLU
Activation function in last layer	SoftMax (Logit)

Table 1. Hyperparameter configuration.

To analyse the trained and tested models, the confusion matrices were determined and from them, accuracy, precision, recall and Area Under the Receiver Operating Characteristic Curve (ROC AUC) were calculated.

4. Results and Discussion

4.1 Dataset

Figure 3 shows some examples of images from the dataset to illustrate the complexity of the data and, consequently, the training and classification issues. Figures 3.a, 3.b and 3.c are examples of images labelled as HLB-infected. Figures 3.d, 3.e and 3.f are examples of images labelled as non-HLB.

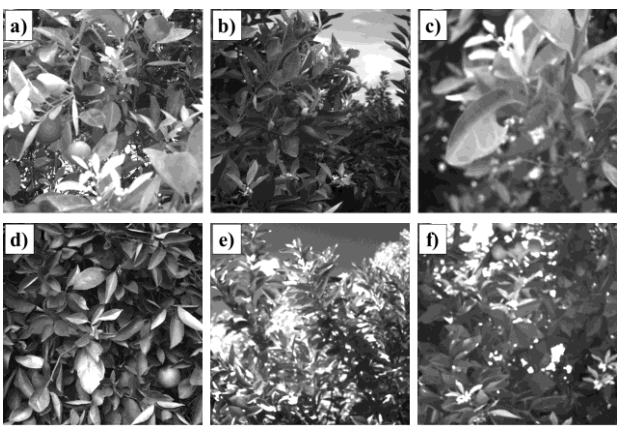

Figure 3. Examples of images from the dataset collected with the 710 nm channel. a) Image with HLB symptoms; b) image with HLB symptoms and sky; c) blurred image with HLB symptoms; d) leaves without HLB symptoms; e) image with leaves without HLB symptoms and sky; and f) blurred image of leaves without HLB symptoms.

Figure 3.a presents symptoms easily visualised in the 710 nm channel image. The image also includes objects such as oranges and wood. Finally, it is possible to observe how some leaves are more illuminated than others. These characteristics in the image illustrates the complexity of the canopy and the challenges that the model may encounter in identifying symptoms within this context. Figure 3.d is an example of an image from non-HLB label and presents leaves, orange, and some stem. The figure also presents the complexity of illumination due to the positions and shapes of the leaves.

This contribution has been peer-reviewed. The double-blind peer-review was conducted on the basis of the full paper.
https://doi.org/10.5194/isprs-annals-X-3-2024-331-2024 | © Author(s) 2024. CC BY 4.0 License.

Figures 3.b and 3.e illustrate the challenge posed by the sky in the images, in addition to symptomatic and non-symtomaitc leaves. These issues reflect a real-world field scenario where backgrounds such as the sky or neighbouring trees from adjacent planting rows are captured by the images. Such occurrences introduce further complexity into the training and classification process.

Figures 3.c and 3.f show blurred images to depict the variability of the data acquisition. The more variability within the training data the more generic the models will become. Blurred images can be common in real-word acqusitions, since wind is very likely to disturb acquisitions and that multispectral sensor have fixed focus. This is a positive point since the spectral dimension cannot be augmented by traditional methods of data augmentation commonly used in preprocessing data to deep neural networks. Therefore, for this dataset the images were acquired varying the camera shutter speed and the camera to the object range. These variations in acquisition produced a "physical augmentation" to the dataset.

HLB citrus image datasets are lacking in the scientific repositories, especially multispectral image datasets. Rauf et al (2016) and Hughes & Salathé (2016) are examples of fruits datasets and repositories, but both included only RGB images and leaves detached from the canopy.

4.2 Training and testing

The training process of the models, as shown in Figure 4, demonstrated consistent improvement over 200 epochs with stable performances after approximately 70 epochs for ResNet18 (Figure 4.a) and after around 90 epochs for ResNet34 (Figure 4.b). Initially, the training loss showed a sharp decline, indicating a phase of rapid learning, while the training accuracy steadily increased, suggesting that the model’s predictions are increasingly aligning with the training dataset. Notably, the training loss for Figure 4.a and Figure 4.b stabilises after 70 and 90 epochs, respectively, while the training accuracy achieved around 90%, which may indicate that the model has reached its learning capacity with the provided data. The results presented in Figure 4 point to a robust learning process.

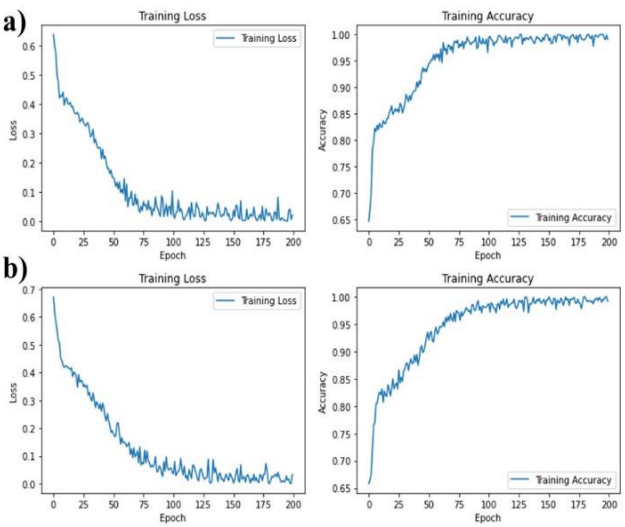

Figure 4. a) Training loss curve and training accuracy curve of ResNet18 and b) Training loss curve and training accuracy curve of ResNet34.

Considering training due to dataset characteristics and the inherent complexities of binary classification (HLB or non-HLB) within a complex canopy environment, the models demonstrate satisfactory performance. Notably, despite the absence of established learning pipelines commonly sutilised in deep learning approaches such as transfer learning and fine tuning (Pan & Yang, 2010), the models still yield promising results.

By analysing the confusion matrices and the metrics derived from them, it is possible to understand the strengths and weaknesses of the models. Figure 5 presents confusion matrices of ResNet18 and ResNet34 after 200 training epochs when tested with the test dataset, which is the data that was not used in model training.

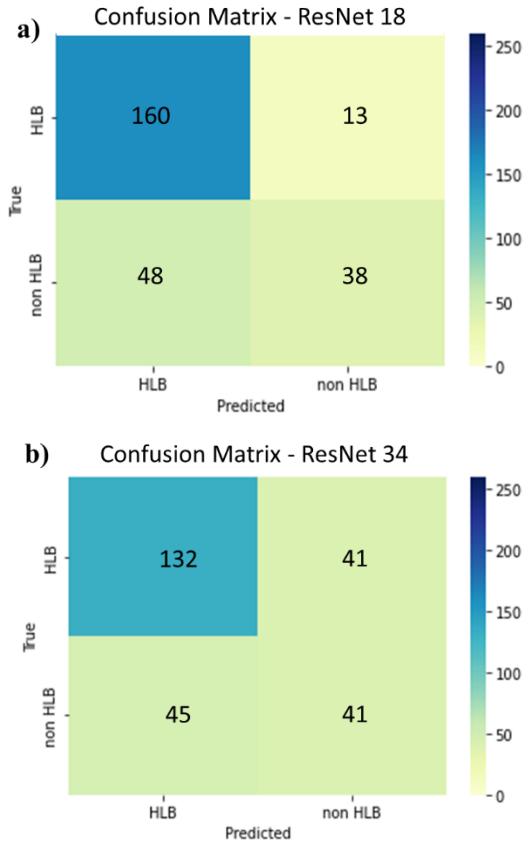

Figure 5. a) Confusion matrix of the ResNet18 and b) Confusion matrix of the ResNet34, both on the test dataset with 200 epochs of training.

From Figure 5.a it can be seen that the main confusion of the ResNet18 model is the false positive of non-HLB samples predicted as HLB. In practice, this shows that the model overestimates the probability of the disease's presence in the canopy. In such a case, a double check on these trees should be conducted to confirm the presence of HLB symptoms. The opposite (false negative predictions) happens with a lesser frequency, i.e. the model rarely labbels infected canopies as healthy ones. This scenario represents where the desired sensitivity, since neglected infected trees can be the focus of a larger dissemination of the HLB on the orchard. From Figure 5.b it can seen that with ResNet34 the number of false positives to HLB is almost the same as ResNet18. However, false negative predictions are significantly higher than in ResNet18. Eventually, the achieved results with ResNet34 model is insufficient and unreliable in the field. With the simpler ResNet18, HLB symptoms are accurately detected within complex canopies, but

the false alarm rate still requires improvements to be considered as a technique to monitoring orchards.

Upon evaluating the performance of the ResNet models with the test dataset, a disparity in accuracy is observed. The ResNet34 model achieved an accuracy of 66.79%, considerably lower than the 76.45% accuracy achieved by the ResNet18 model (Table 2). This validates the indication of the better performance of the ResNet18.

		ResNet18	ResNet34
Accuracy		76.45%	66.79%
ROC AUC		68.34%	61.99%
Precision	HLB	76.92%	74.58%
	Non-HLB	74.51%	50%
Recall	HLB	92.48%	76.30%
	Non-HLB	44.19%	47.67%

Table 2. Evaluated performance of the models on the test dataset with 200 epochs of training.

The ROC AUC provides an overall assessment of the model's ability to distinguish between classes. This is particularly useful as an overview of model performance. Table 2 shows the ROC AUC for the models. ROC AUC of ResNet18 suggests a model with a moderate capacity to distinguish the classes; 68.34% of the time, the model will correctly classify a positive instance as more likely to be positive than a negative instance. However, ROC AUC of ResNet34 (61.99%) suggests a model with some discrimination capability but only a slightly better skill than a random classifier (50%). This performance suggests that the model may not be extracting features in the data efficiently.

Precision is the rate of true positives regarding the total of positives predicted. ResNet18 presents similar precision in two classes: 76.92% and 74.51% to HLB and non-HLB, respectively. However, the precision with ResNet34 was not similar between classes: 74.58% to HLB and 50% to non HLB.

Recall is the rate of true positives regarding the total of cases truly positives. The recall for the test of ResNet18 is 92.48% for HLB and 44.19% for non-HLB class. This means that in 92.48% of the cases that the model predicts an image as HLB, the prediction is correct, which is a high rate of correction predictions. However, this rate is significantly lower for non-HLB class, achieving 44.19%. These results can be attributed to the unbalanced dataset, since HLB class has more images than non-HLB class. ResNet34 model test presented recall results of 76.30% and 47.67% to HLB and non-HLB, respectively. Again, the imbalance between classes is evident. Furthermore, the ResNet18 presented an improved performance, which was coherent with accuracy, precision and ROC AUC.

This result suggests that ResNet18, with fewer layers, outperformed its more complex counterpart in the test dataset. These findings leads to a deeper investigation into the efficiency of the models' architectures, the possibilities of overfitting, and the complexity of the dataset. The superior accuracy of ResNet18 might indicate that, when dealing with the provided test dataset, a less complex model with fewer convolutional layers is more ffective, possibly due to better generalisation and prevention of overfitting.

4.3 Comparative analysis of results

In the background literature, despite the high accuracy values, all focus on detecting the disease was given on using an isolated leaf from the tree. In our work, we aimed to apply binary disease classification in a more complex context with part of the citrus tree and various situations, such as low lighting, high lighting, shadow, and object overlap, containing parts of the sky in the image, as highlighted in Figure 3.b.

For the detection of HLB in citrus, Farzaneh et al. (2019) investigated the possibility of using image data collected by UAVs, combined with 16 vegetation indices, achieving 81.75% of accuracy in identifying healthy and diseased trees. They also concluded that it is necessary to explore more advanced machine learning algorithms for classification tasks in multispectral image analysis.

In 2024, the Institute of Food and Agricultural Sciences (IFAS), affiliated with the University of Florida, published a citrus production guide for the years 2023-2024 (Kadyampakeni and Duncan, 2023). This guide covers the main symptoms that can be easily confused with other diseases, such as citrus rust, Phytophthora root rot, and waterlogging.

Therefore, diagnosing HLB based solely on symptoms becomes a labour-intensive and time-consuming task. Currently, in large plantations, the work is performed by trained technicians who can make this labbeling. However, even experienced individuals may make mistakes due to fatigue and long hours under the sun.

Using image detection for disease identification would allow farmers to pinpoint affected areas in their crops with less human labour, achieving an accuracy rate of 76.45%, as demonstrated by the model. This method could enable disease management through imagery, reducing human fatigue and analytical bias.

Currently, this is the only comparative detection rate study for HLB (citrus greening) using this technique, as field assessments are still conducted manually. The success rate can be compared to other crops, emphasising the benefits of automated image analysis in agriculture.

5. Final Considerations

The present study introduces an investigation aimed at assessing the feasibility of employing the deep neural network ResNet for the binary classification of HLB disease in orange trees utilising multispectral images. These images were captured under *in situ* conditions in a young orange orchard on a commercial farm.

The dataset reveals the challenges associated with identifying HLB symptoms within citrus canopies using multispectral imaging. The complexity of the canopy environment is evident, with variations in natural illumination and the presence of other objects, such as oranges and wood, which can potentially obstruct the symptoms. Additionally, real-world field complexities during data acquisition, such as the presence of sky in the image, variations in image lighting, and blur induced by environmental factors like wind, further complicate the analysis. Notably, the dataset's inclusion of such variability through augmentation via variations in shutter speed and acquisition distance enhances its representativeness, facilitating more robust model training. Moreover, the scarcity of multispectral datasets tailored

specifically to HLB citrus imagery underscores the novelty and importance of this work.

However, the use of ResNet18 and ResNet34 showcased optimistic performance even with limited training data, rendering it especially valuable for tasks involving small datasets, a frequent scenario in the domain of multispectral imagery analysis. Finally, contrary to expectations, ResNet18 results in a higher accuracy and, in general, better performance evaluation compared to ResNet34. These results suggest that a model with fewer convolutional layers is more effective, potentially attributed to an improved generalisation and the mitigation of overfitting. Moreover, the results indicate that deep neural network approaches can adeptly handle non-radiometric calibrated data and discern differences between HLB and non-HLB images.

As a perspective to improve the robustness of the models, image augmentation (channel by channel since is not possible spectral augmentation) and more *in situ* data collection will be conducted. In addition, reducing the spectral dimension with band selection, vegetation index and PCA can turn feasible a form of transfer-learning and/or fine-tuning. Sharma & Ross (2020) suggest augmenting the weights trained on the ImageNet database to adapt them to the dimensions of different spectral images and use them as initial conditions to retrain standard backbones or fine-tune them.

Future works will be directed at confirming the results with svisualise attention maps to "understand" which visual artefacts will provide qualitative understanding of the relationship between patches in an image and the model's prediction (Ribeiro et al., 2016).

Acknowledgements

This study was financed in part by the Coordenação de Aperfeiçoamento de Pessoal de Nível Superior – Brasil (Grants nº: 88887.839524/2023-00, 88887.817757/2023-00 and 88887.840159/2023-00); by São Paulo Research Foundation - FAPESP (Grant nº: 2021/06029-7), and by Conselho Nacional de Desenvolvimento Científico e Tecnológico - CNPq, (Grants: 308747/2021-6 and 303670/2018-5).

References

Agrowing, 2024. Agrowing Sensors [WWW Document]. URL http://www.agrowing.com/

Ahmed M., Ahmed A., 2023. Palm tree disease detection and classification using residual network and transfer learning of inception ResNet. PLoS ONE 18(3): e0282250. https://doi.org/10.1371/journal.pone.0282250

Alquezar, B., Carmona, L., Bennici, S., Miranda, M. P., Bassanezi, R. B., & Peña, L., 2022. Cultural Management of Huanglongbing: Current Status and Ongoing Research. In Phytopathology (Vol. 112, Issue 1, pp. 11–25). *American Phytopathological Society*. https://doi.org/10.1094/PHYTO-08-21-0358-IA

Aquino, A., Millan, B., Diago, M. P., & Tardaguila, J., 2018. Automated early yield prediction in vineyards from on-the-go image acquisition. *Computers and Electronics in Agriculture*, 144, 26–36. https://doi.org/10.1016/j.compag.2017.11.026

Barbedo, J. G. A., Koenigkan, L. V., Vieira, B. de A. H., Costa, R. V., Nechet, K. de L., Godoy, C. V., Junior, M. L., Patrício, F. R. A., Talamini, V., Chitarra, L. G., Oliveira, S. A. S. de, Ishida, A. K. N., Fernandes, J. M. C., Santos, T. T., Cavalcanti, F. R., Terao, D., & Angelotti, F., 2018. Annotated Plant Pathology Databases for ImageBased Detection and Recognition of Diseases. 16, 1749–1757.

Bové, J. M., 2006. Huanglongbing: A Destructive, Newly-Emerging, Century-Old Disease Of Citrus. In Source: *Journal of Plant Pathology* (Vol. 88, Issue 1).

Deery, D., Jimenez-Berni, J., Jones, H., Sirault, X., & Furbank, R., 2014. Proximal remote sensing buggies and potential applications for field-based phenotyping. In *Agronomy* (Vol. 4, Issue 3, pp. 349–379). MDPI. https://doi.org/10.3390/agronomy4030349

Deng, X., Huang, Z., Zheng, Z., Lan, Y., & Dai, F., 2019. Field detection and classification of citrus Huanglongbing based on hyperspectral reflectance. *Computers and Electronics in Agriculture*, 167. https://doi.org/10.1016/j.compag.2019.105006

Dhiman, P.; Kaur, A.; Hamid, Y.; Alabdulkreem, E.; Elmannai, H.; Ababneh, N., 2023. Smart Disease Detection System for Citrus Fruits Using Deep Learning with Edge Computing. *Sustainability*, 15, 4576. https://doi.org/10.3390/su15054576

Farzaneh, DadrasJavan., Farhad, Samadzadegan., Seyed, Hossein, Seyed, Pourazar., Haidar, Fazeli., 2019. UAV-based multispectral imagery for fast Citrus Greening detection. *Journal of Plant Diseases and Protection*, 126(4):307-318. doi: 10.1007/S41348-019-00234-8

Fundecitrus., 2023. Levantamento da incidência das doenças dos citros: greening, cvc e cancro cítrico no cinturão citrícola de São Paulo e Triângulo/Sudoeste Mineiro 2023. www.fundecitrus.com.br

Garcia-Ruiz, F., Sankaran, S., Maja, J. M., Lee, W. S., Rasmussen, J., & Ehsani, R., 2013. Comparison of two aerial imaging platforms for identification of Huanglongbing-infected citrus trees. *Computers and Electronics in Agriculture*, 91, 106–115. https://doi.org/10.1016/j.compag.2012.12.002

He, K., Zhang, X., Ren, S., & Sun, J., 2016. Deep Residual Learning for Image Recognition. *Proceedings of the IEEE conference on computer vision and pattern recognition*. Las Vegas, NV, USA, pp. 770-778. https://doi.org/10.1109/CVPR.2016.90.

Hughes, D. P., & Salathé, M., 2016. An open access repository of images on plant health to enable the development of mobile disease diagnostics. https://doi.org/10.48550/arXiv.1511.08060

Kadyampakeni, D., & Duncan, L., 2023. Florida Citrus Production Guide: Best Management Practices for Soil-Applied *Agricultural Chemicals*: CPG ch. 6, CG027/HS-185, rev. 5/2023. EDIS. https://doi.org/10.32473/edis-cg027-2023

Kamilaris, A., & Prenafeta-Boldú, F. X., 2018. Deep learning in agriculture: A survey. *Computers and electronics in agriculture*, 147, 70-90.

Pan, S. J., & Yang, Q. , 2009. A survey on transfer learning. *IEEE Transactions on knowledge and data engineering*, 22(10), 1345-1359. https://doi.org/10.1109/TKDE.2009.191

Qiu R-Z, Chen S-P, Chi M-X, Wang R-B, Huang T, Fan G-C, Zhao J and Weng Q-Y., 2022. An automatic identification system for citrus greening disease (Huanglongbing) using a YOLO convolutional neural network. *Front. Plant Sci*. 13:1002606. https://doi.org/10.3389/fpls.2022.1002606

Rançon, F., Keresztes, B., Deshayes, A., Tardif, M., Abdelghafour, F., Fontaine, G., Da Costa, J. P., & Germain, C., 2023. Designing a Proximal Sensing Camera Acquisition System for Vineyard Applications: Results and Feedback on 8 Years of Experiments. *Sensors*, 23(2). https://doi.org/10.3390/s23020847

Rangarajan, A K.., & Purushothaman, R., 2020. Disease Classification in Eggplant Using Pre-trained VGG16 and MSVM. Sci Rep 10, 2322. https://doi.org/10.1038/s41598-020-59108-x

Rauf, H. T., Saleem, B. A., Lali, M. I. U., Khan, M. A., Sharif, M., & Bukhari, S. A. C., 2019. A citrus fruits and leaves dataset for detection and classification of citrus diseases through machine learning. *Data in Brief*, 26. https://doi.org/10.1016/j.dib.2019.104340

Ribeiro, M. T., Singh, S., & Guestrin, C., 2016. " Why should i trust you?" Explaining the predictions of any classifier. In *Proceedings of the 22nd ACM SIGKDD international conference on knowledge discovery and data mining* (pp. 1135-1144).

Sankaran, S., Maja, J. M., Buchanon, S., & Ehsani, R., 2013. Huanglongbing (Citrus Greening) detection using visible, near infrared and thermal imaging techniques. *Sensors* (Switzerland), 13(2), 2117–2130. https://doi.org/10.3390/s130202117

Shafik, W., Tufail, A., De Silva Liyanage, C. et al., 2024. Using transfer learning-based plant disease classification and detection for sustainable agriculture. *BMC Plant Biol* 24, 136. https://doi.org/10.1186/s12870-024-04825-y

Sharma, Y. & Ross, R., 2020. "Less is More when Applying Transfer Learning to Multispectral Data.” IN: Irish *Conference on Artificial Intelligence and Cognitive Science* (pp. 301-312).

Underwood, J. P., Hung, C., Whelan, B., & Sukkarieh, S., 2016. Mapping almond orchard canopy volume, flowers, fruit and yield using lidar and vision sensors. *Computers and Electronics in Agriculture*, 130, 83–96. https://doi.org/10.1016/j.compag.2016.09.014

Wendel, A., & Underwood, J., 2017. Illumination compensation in ground based hyperspectral imaging. *ISPRS Journal of Photogrammetry and Remote Sensing*, 129, 162–178. https://doi.org/10.1016/j.isprsjprs.2017.04.010

Wendel, A., Underwood, J., & Walsh, K., 2018. Maturity estimation of mangoes using hyperspectral imaging from a ground based mobile platform. *Computers and Electronics in Agriculture*, 155, 298–313. https://doi.org/10.1016/j.compag.2018.10.021

Wold, Svante, 1995. Chemometrics; what do we mean with it, and what do we want from it? *Chemometrics and intelligent laboratory systems*, v. 30, n. 1, p. 109-115. ISSN 0169-7439, doi: 10.1016/0169-7439(95)00042-9

Yang D, Wang F, Hu Y, Lan Y and Deng X., 2021. Citrus Huanglongbing Detection Based on Multi-Modal Feature Fusion Learning. *Front. Plant Sci*. 12:809506. https://doi.org/10.3389/fpls.2021.809506